Totally Blind APP Channel Estimation with Higher Order Modulation Schemes

Frieder Sanzi
Institute of Telecommunications,
University of Stuttgart
Pfaffenwaldring 47, D-70569 Stuttgart, Germany
Email: sanzi@inue.uni-stuttgart.de
Tel.: +49 711 685 7941 Fax: +49 711 685 7929

Marc C. Necker
Institute of Communication Networks and Computer Engineering,
University of Stuttgart
Pfaffenwaldring 47, D-70569 Stuttgart, Germany
Email: necker@ikr.uni-stuttgart.de
Tel.: +49 711 685 7963 Fax: +49711 685 7983

***Abstract*— A new two-dimensional blind channel estimation scheme for coherent detection of OFDM signals in a mobile environment is presented. The channel estimation is based on the A Posteriori Probability (APP) calculation algorithm. The time-variant channel transfer function is completely recovered without phase ambiguity with no need for *any* pilot or reference symbols. The two-dimensional channel estimation is performed by applying a concatenation of two one-dimensional APP estimators for frequency and time direction in combination with an iterative estimation and decoding loop. The phase ambiguity problem is solved by using higher order modulation schemes with asymmetrical arrangement. The proposed approach maximizes the spectral efficiency by avoiding any reference or pilot symbols and minimizes the BER by using coherent demodulation. We investigate the performance of our algorithm with respect to the BER and study the convergence of the iterative estimation and decoding loop using Extrinsic Information Transfer (EXIT) charts.**

I. Introduction

Time varying propagation conditions make channel estimation (CE) a demanding task at the receiver. In OFDM, the two-dimensional channel transfer function (CTF) must be estimated if coherent detection is used. This is often achieved by inserting pilot symbols into the transmitted signal and cascading two one-dimensional FIR interpolation filters at the receiver [1].

Blind channel estimation algorithms make pilot symbols unnecessary. They are often based on higher order statistics and converge slowly, making them unsuitable for mobile environments and for burst reception. Additionally, a phase ambiguity is introduced in the channel estimate. At least one reference symbol is necessary to resolve this phase ambiguity if coherent demodulation is desired. Alternatively, differentially coherent demodulation can be used. This, however, leads to loss in E_b/N_0 of approximately 2 dB for AWGN channels and larger losses for fading channels [2].

In [3] the authors present a fast converging blind channel estimator based on the Maximum Likelihood principle, which recovers the amplitude and phase of a channel without the need for any reference symbols. This is achieved by combining modulation schemes, such as QPSK and 3-PSK.

Another method to estimate the channel is based on the calculation of the A Posteriori Probability (APP) [4]. The two-dimensional CTF is estimated by concatenating two 1-dimensional APP estimators in frequency and time direction, respectively. This method dramatically reduces the amount of pilot symbols compared to FIR interpolation. Furthermore, the APP channel estimator can be embedded in an iterative decoding loop with a soft in/soft out decoder.

In this paper we combine the idea of totally blind and APP channel estimation (APP-CE). We use modulation schemes with an asymmetrical arrangement to solve the phase ambiguity problem. The performance is evaluated with a fast-varying mobile channel on the basis of BER charts and the Extrinsic Information Transfer chart (EXIT chart) [5].

The remainder of this paper is structured as follows. In section II the system model is presented. Section III derives the totally blind APP channel estimation algorithm. Finally, section IV presents the simulation results.

II. System Model

A. Transmitter and Receiver

We investigate an OFDM-system with $K = 1000$ subcarriers having a carrier-spacing of 4 kHz and an OFDM-symbol duration of $T_s = 312.5\,\mu$s. $L = 100$ successive OFDM symbols are combined for blockwise transmission. The signal from the binary source is convolutionally encoded and interleaved as shown in Fig. 1. After interleaving, three successive coded bits are grouped and mapped onto an 8-ary symbol $X_{k,l}$. The signal $X_{k,l}$ is modulated onto K orthogonal sub-carriers by an iFFT-block. Finally, a cyclic prefix of length 1/4 is inserted.

At the receiver, an iterative APP-CE is applied [4]. We obtain the received 8-ary signal constellation points $Y_{k,l}$ after

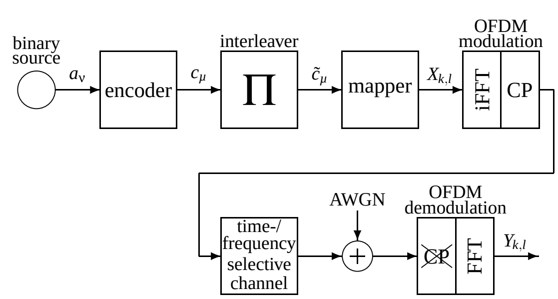

Fig. 1: Transmitter and channel model.

IEEE Vehicular Technology Conference (VTC), Orlando, USA, October 2003

removal of the cyclic prefix and OFDM demodulation:

$$Y_{k,l} = H_{k,l} \cdot X_{k,l} + N_{k,l}, \tag{1}$$

where l is the OFDM symbol index, k is the sub-carrier index and $N_{k,l}$ are statistically i.i.d. complex Gaussian noise variables with component-wise noise power $\sigma_N^2 = N_0/2$. The $H_{k,l}$ are sample values of the CTF:

$$H_{k,l} = H(k \cdot \Delta f, l \cdot T_\mathrm{s}), \tag{2}$$

whereby Δf is the sub-carrier spacing and T_s is the duration of one OFDM symbol (useful part plus guard interval).

The signal $Y_{k,l}$ is fed to the blind APP-CE stage as shown in Fig. 2. This stage outputs log-likelihood ratios (L-values) on the transmitted coded bits which are deinterleaved and decoded in an APP decoder. Iterative channel estimation and decoding is performed by feeding back extrinsic information on the coded bits; after interleaving it becomes the *a-priori* knowledge to the blind APP-CE stage. The APP-CE stage is explained in detail in section III-A.

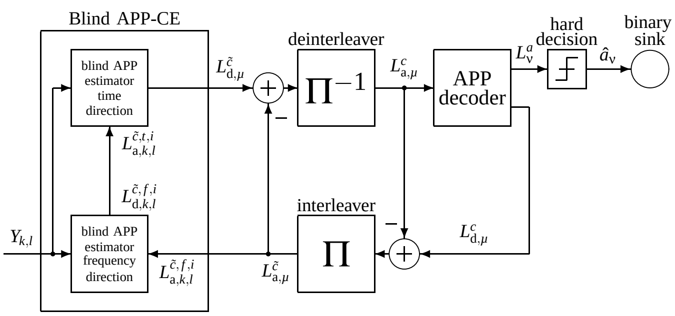

Fig. 2: Receiver with iterative blind APP channel estimation.

B. Channel Model

For the performance evaluation of the blind channel estimator we assumed a frequency-selective fading channel according to a wide-sense stationary uncorrelated scattering (WSSUS) model. A Jakes-distribution was assumed for the Doppler spectrum with $f_{\mathrm{D}_\mathrm{max}} = 100\,\mathrm{Hz}$ and an exponentially decaying distribution for the power delay profile with $\tau_\mathrm{max} = 20\,\mu\mathrm{s}$.

The WSSUS-channel was simulated according to the model introduced in [6], which describes the channel's time-variant impulse response as

$$h(\tau, t) = \lim_{Z\to\infty} \frac{1}{\sqrt{Z}} \sum_{m=1}^{Z} e^{j\theta_m} e^{j2\pi f_{\mathrm{D}m} t} \delta(\tau - \tau_m) \ . \tag{3}$$

The Fourier-Transform of equation (3) with respect to τ yields the channel's time-variant frequency response:

$$H(f, t) = \lim_{Z\to\infty} \frac{1}{\sqrt{Z}} \sum_{m=1}^{Z} e^{j\theta_m} e^{j2\pi f_{\mathrm{D}m} t} e^{-j2\pi f \tau_m} \ . \tag{4}$$

For each of the Z paths, the phase-shift θ_m, the Doppler-shift f_{D_m} and the delay τ_m are randomly chosen from the corresponding probability density function $p_\theta(\theta)$, $p_{f_\mathrm{D}}(f_\mathrm{D})$ or $p_\tau(\tau)$ of the channel model [6]. For the simulations, the number of paths was chosen to be $Z = 100$, which is a good tradeoff between simulation speed and accuracy.

III. Totally Blind APP Channel Estimation

A. APP Channel Estimation

The two-dimensional blind APP channel estimator consists of two estimators for frequency and time direction, respectively [4]. The estimation algorithm exploits the time and frequency continuity of the CTF at the receiver.

For one-dimensional APP estimation, the symbol-by-symbol MAP-algorithm is applied with an appropriately chosen metric. To help understanding, the symbols $X_{k,l}$ at the transmitter in Fig. 1 can be thought of being put into a virtual shift register at the output of the mapper. Owing to this "artificial grouping", the corresponding trellis exploits the time and frequency continuity of the CTF at the receiver.

At frequency index k, the APP estimation in frequency direction is characterized for OFDM symbol l_0 with $0 \le l_0 \le L-1$ by the metric increment

$$\gamma_k = -\frac{|Y_{k,l_0} - \hat{H}^f_{k,l_0} \cdot \hat{X}_{k,l_0}|^2}{2 \cdot \sigma_f^2} + \sum_{i=0}^{2} d^i_{k,l_0} \cdot L^{\tilde{c},f,i}_{\mathrm{a},k,l_0} \tag{5}$$

with estimated channel coefficient

$$\hat{H}^f_{k,l_0} = \sum_{i=1}^{m_f} u_{f,i} \cdot \frac{Y_{k-i,l_0}}{\hat{X}_{k-i,l_0}}, \tag{6}$$

whereby the FIR filter coefficients $u_{f,i}$ are calculated with the Wiener-Hopf equation based on the frequency auto-correlation function $R_{f;\Delta k}$ [4] and m_f is the prediction order. The $\hat{X}_{k,l_0}$ denote the hypothesized transmitted data symbol according to the trellis structure. For the calculation of the prediction coefficients $u_{f,i}$, we assume that the current state was transmitted. Under this assumption, (6) can be expressed as

$$\hat{H}^f_{k,l_0} = \sum_{i=1}^{m_f} u_{f,i} \cdot \hat{H}_{k-i,l_0} \ , \tag{7}$$

whereby

$$\hat{H}_{k-i,l_0} = H_{k-i,l_0} + \frac{N_{k-i,l_0}}{\hat{X}_{k-i,l_0}} \ . \tag{8}$$

Taking (8) into account, we can compute the expected value

$$\mathrm{E}\left\{\hat{H}_{k-i,l_0} \cdot \hat{H}^*_{k-\tilde{i},l_0}\right\} = R_{f;\tilde{i}-i} + \delta_{\tilde{i}-i} \cdot \frac{N_0}{\left|\hat{X}_{k-i,l_0}\right|^2} \ , \tag{9}$$

with

$$R_{f;\tilde{i}-i} = \mathrm{E}\left\{H_{k-i,l_0} \cdot H^*_{k-\tilde{i},l_0}\right\} \ , \tag{10}$$

whereby * denotes conjugate operation and δ_k is the Kronecker symbol.

The $L^{\tilde{c},f,i}_{\mathrm{a},k,l_0}$ in (5) are the *a priori* L-values of the coded bits $\tilde{c}_\mu$ which are fed to the APP estimator in frequency direction. The bits d^0_{k,l_0}, d^1_{k,l_0} and d^2_{k,l_0} in the sum in (5) result from the hard demapping of $\hat{X}_{k,l_0}$. The term $2\sigma_f^2$ is the variance of the estimation error in frequency direction according to [7]. The

APP estimation in time direction is done in a similar way for each sub-carrier taking into account the time auto-correlation function $R_{t;\Delta l}$ of the CTF [4]. The two one-dimensional APP estimators are concatenated as shown in Fig. 2. The output $\tilde{L}^{c,f,i}_{\mathrm{d},k,l}$ of the APP estimator in frequency direction becomes the *a priori* input $\tilde{L}^{c,t,i}_{\mathrm{a},k,l}$ of the APP estimator in time direction. The prediction order for estimation in frequency and time direction, respectively, was chosen to be 2 for our simulations.

B. Totally Blind Channel Estimation

The totally blind channel estimation algorithm in [3] is based on the Maximum Likelihood (ML) principle as presented in [8]. One of the key problems is the following maximization equation, which needs to be solved:

$$\hat{\Psi} = \min_{\Psi} \|\mathbf{y} - \mathbf{X}\mathbf{A}_d\mathbf{h}\|^2 \quad , \quad \Psi := [\mathbf{h}^T, \mathbf{x}^T]^T \ . \tag{11}$$

$\mathbf{h}$ is a vector of taps for the discrete-time channel impulse response. $\mathbf{x}$ and $\mathbf{y}$ are vectors with M symbols transmitted and received on adjacent subcarriers, respectively. $\mathbf{X}$ is a diagonal matrix containing the corresponding transmitted data symbols as diagonal elements. $\mathbf{A}_d$ is the DFT matrix, where

$$\begin{aligned} \mathbf{A}_d &= [\mathbf{a}_{d,0} \ \mathbf{a}_{d,1} \ \cdots \ \mathbf{a}_{d,G-1}] \ , \\ \mathbf{a}_{d,m} &= [1 \ e^{-jm\Delta\omega T_s} \ \cdots \ e^{-jm\Delta\omega T_s(M-1)}]^T \ , \end{aligned} \tag{12}$$

with T_s being the duration of one data symbol and $\Delta\omega$ the subcarrier spacing $\Delta\omega = 2\pi/KT_s$.

In [8], the authors used exhaustive search and a branch-and-bound integer programming strategy to solve the maximum equation (11). In [3], the autocorrelation of the channel transfer function in frequency direction was taken advantage of in order to reduce the number of elements in the vectors and matrices of (11). It was shown that as few as two data symbols on adjacent subcarriers are sufficient to estimate the channel transfer function, which makes it trivial to solve (11). A suboptimal approach was presented which significantly reduces the complexity of the optimization problem when more than two subcarriers are considered.

One of the major contributions of [3] was the resolution of the phase ambiguity of the channel estimate without the help of any pilots or reference symbols, even in fast varying mobile environments. This was realized by using two different PSK-modulation schemes on adjacent subcarriers. Let q_i be a signal point of the first PSK-modulation scheme and q_j a signal point of the second modulation scheme. If $\alpha_{i,j} = \angle(q_i, q_j)$ denotes the angle between both signal points in the complex plane, the signal points of the modulation schemes must be chosen such that no two angles $\alpha_{i,j}$ are identical for all possible signal point combinations i, j. For example, QPSK and 3-PSK fulfill this condition.

If the channel transfer function does not vary fast in frequency direction (i.e. the autocorrelation fulfills certain conditions), the receiver can determine the symbols $X_{k,l}$ and $X_{k+1,l}$ sent on adjacent subcarriers without any ambiguity [3]. Simulations showed that this concept delivers good BER-performance with COST207-channels RA and TU. For channels with longer delay spreads, this concept imposes problems as the condition of a slow varying CTF in frequency direction only holds for some subcarriers.

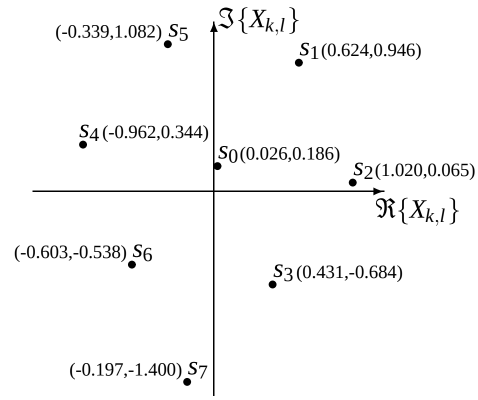

Fig. 3: Minimum-error 8-ary modulation scheme.

C. Iterative totally blind APP Channel Estimation

The APP channel estimator can be used to efficiently solve the maximum equation (11) under consideration of an appropriately chosen metric. Using this trellis based approach, we can obtain an excellent solution and at the same time greatly reduce the complexity of the optimization problem.

If we use regular 8-QAM, the APP channel estimator as described in section III-A still needs pilot symbols as any symbol sequence $e^{j\tilde{\varphi}}\hat{X}_{k,l}$, $\tilde{\varphi} = 0, \frac{1}{2}\pi, \pi, \frac{3}{2}\pi$, is a possible solution for the APP channel estimator. It is obvious that a combination of modulation schemes as described in the previous section will resolve this phase blindness and make the pilots unnecessary.

In contrast to the approach in [3] where blocks of 10 data symbols within one OFDM symbol were considered, the APP estimator considers a much longer sequence of data symbols. This sequence length is on the order of several thousand data symbols. Instead of using two different modulation schemes on adjacent subcarriers, it is therefore possible to get along with only one modulation scheme and still be able to resolve the phase blindness. In order to achieve this, the modulation schemes must be asymmetrical. In this case, and if not all sent symbols are identical[1], there is only one possible phase $\tilde{\varphi}$ yielding a valid solution in the APP channel estimation stage. Hence, the phase of the channel estimate is successfully restored without the help of pilots or reference symbols. Since the APP channel estimator performs with very little *a-priori* knowledge, it will now be possible to also estimate fast-varying channels with a long delay spread, such as COST207 HT.

For our system, we use the asymmetrical zero-mean 8-ary minimum-error signal constellation presented in [9] and shown in Fig. 3. As a consequence of this asymmetrical signal constellation, the symbols in Fig. 3 have different absolute values.

[1]It is most likely that all symbols from the symbol alphabet occur with equal probability in the considered symbol sequence due to the application of error correcting codes.

This aspect has to be taken into account for the calculation of the predictor coefficients in section III-A, (9). Therefore, each state of the trellis has its own predictor coefficients.

D. Mapping

The asymmetrical constellation in Fig. 3 was derived in [9] and found to give minimum symbol error performance among all 8-QAM constellations. Let $\mathcal{S} = \{s_0, s_1, \ldots, s_7\}$ be the symbol alphabet as shown in Fig. 3 with $X_{k,l} \in \mathcal{S}$. Let further $\mathcal{B} = \{b_0, b_1, \ldots, b_7\}$ be the set of bit vectors that need to be mapped to the symbol alphabet, where $b_i \in \{000_2, 001_2, \ldots, 111_2\}$. If $\mathcal{M} : \mathcal{B} \to \mathcal{S}$ denotes the mapping from the bit vectors to the signal points, there are 7! different mappings $\mathcal{M}$ (Note that there are 8 equivalent permutations of each mapping).

For the remainder of the paper, we define the following four mappings, for which the EXIT charts (see below) are most promising:

- Mapping $\mathcal{M}0$ (from [10]):
  $\mathcal{B}_0 = \{000_2, 001_2, 010_2, 011_2, 100_2, 101_2, 110_2, 111_2\}$
- Mapping $\mathcal{M}1$:
  $\mathcal{B}_1 = \{000_2, 011_2, 101_2, 110_2, 001_2, 010_2, 100_2, 111_2\}$
- Mapping $\mathcal{M}2$:
  $\mathcal{B}_2 = \{000_2, 101_2, 010_2, 111_2, 011_2, 110_2, 100_2, 001_2\}$
- Mapping $\mathcal{M}3$:
  $\mathcal{B}_3 = \{000_2, 110_2, 010_2, 011_2, 101_2, 100_2, 001_2, 111_2\}$

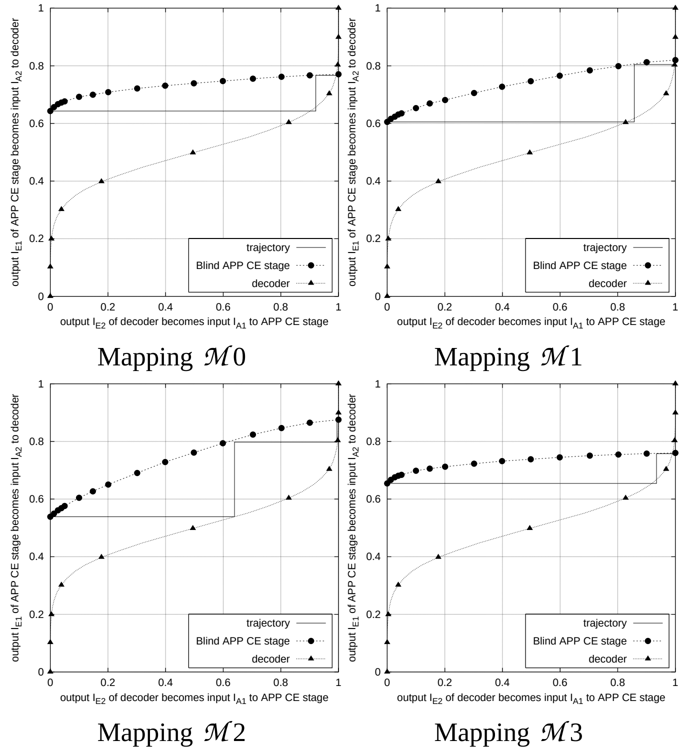

Fig. 4: EXIT chart, blind APP-CE stage and decoder with simulated trajectory of the iterative decoding loop at $E_b/N_0 = 9\,$dB.

IV. Simulation results

The convergence behavior of the iterative decoding loop can conveniently be investigated using EXIT charts [5], which are shown in Fig. 4 for the four mappings $\mathcal{M}0$ through $\mathcal{M}3$ and $E_b/N_0 = 9\,$dB.

The EXIT charts contain the characteristic curves of the blind APP-CE stage and the convolutional decoder. The trajectory shows the exchange of information between the blind APP-CE stage and the decoder. The characteristics of the EXIT charts reflect itself in the BER performance, which is shown in Fig. 5 before the start of the iteration loop and after one, two and three iterations.

For mapping $\mathcal{M}2$, the characteristic curve of the APP stage starts at a mutual information of $I_{E1} \approx 0.54$ at $I_{A1} = 0$. For mappings $\mathcal{M}0$ and $\mathcal{M}3$, the characteristic curves start with a larger $I_{A2} \approx 0.65$. Hence, with no iterations and at an E_b/N_0 of 9 dB, the BER performance of mappings $\mathcal{M}0$ and $\mathcal{M}3$ is about one magnitude better compared to mapping $\mathcal{M}2$.

On the other hand, the characteristic curves of the APP-CE stage and the convolutional decoder intersect at a large mutual information of $I_{E1} \approx 0.87$ for mapping $\mathcal{M}2$, where the curves for mappings $\mathcal{M}0$ and $\mathcal{M}3$ intersect at $I_{E1} \approx 0.77$. Looking at the trajectories, it takes two iterations for mapping $\mathcal{M}2$ and one iteration for mappings $\mathcal{M}0$ and $\mathcal{M}3$ to reach this intersection point. Likewise, after two iterations, the BER performance at $E_b/N_0 = 9\,$dB with mapping $\mathcal{M}2$ becomes better than the BER performance with mappings $\mathcal{M}0$ and $\mathcal{M}3$.

We can also see that optimum BER performance is already achieved after only one or two iterations, depending on the trajectories in the EXIT charts.

Fig. 6 compares the BER of the totally blind APP channel estimator and the pilot-assisted APP channel estimator as used in [4]. The graph shows that for both considered mappings the performance of the blind and the pilot-aided estimator is about the same within the error bars. However, a higher spectral efficiency is achieved with the blind system, since all subcarriers contain useful data symbols.

Note that the receiver decodes blocks of 100 OFDM-symbols with a total duration of 31.25 ms. Results from [11] with pilot-assisted APP channel estimation indicate that excellent BER performance is achievable even for much smaller block sizes. Hence, the totally blind APP channel estimator is not only suitable for broadcasting systems. It is also well suitable for mobile communication systems where the transmission and reception of short data bursts is necessary.

V. Conclusion

The concept of totally blind channel estimation was successfully applied to APP channel estimation. The result is a true blind channel estimator, which is capable of estimating the time-variant channel transfer function including its absolute phase. This is achieved without the need for *any* reference symbols, thus maximizing the spectral efficiency of the underlying OFDM system. Our results clearly indicate that totally blind channel estimation is possible for virtually any realistic time-variant mobile channel.

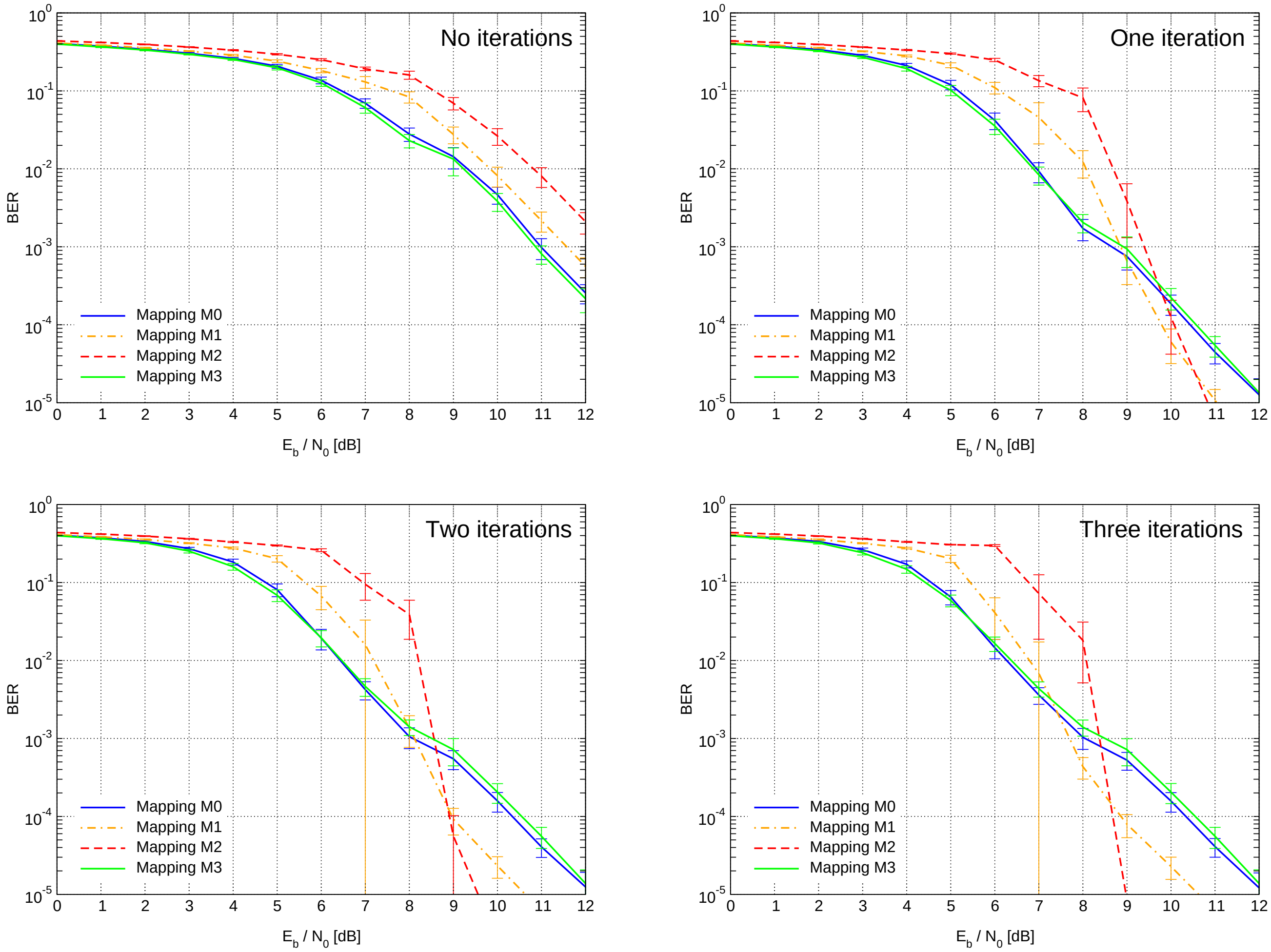

Fig. 5: BER performance of the four mappings after no, one, two and three iterations.

REFERENCES

[1] P. Höher, S. Kaiser, and P. Robertson, "Two–dimensional pilot–symbol–aided channel estimation by Wiener filtering," in *ICASSP*, Munich, Germany, April, 1997, pp. 1845–1848.

[2] J. G. Proakis, *Digital Communications*. McGraw-Hill, 1995.

[3] M. C. Necker and G. L. Stüber, "Totally blind channel estimation for OFDM over fast varying mobile channels," in *Proc. IEEE Intern. Conf. on Comm.*, New York, USA, April, 2002, pp. 421–425.

[4] F. Sanzi and S. ten Brink, "Iterative channel estimation and decoding with product codes in multicarrier systems," in *Proc. IEEE Vehicular Tech. Conf.*, Boston, USA, September, 2000, pp. 1338–1344.

[5] S. ten Brink, "Convergence behavior of iteratively decoded parallel concatenated codes," *IEEE Trans. on Comm.*, vol. 49, no. 10, pp. 1727–1737, October, 2001.

[6] P. Höher, "A statistical discrete-time model for the WSSUS multipath channel," *IEEE Trans. on Veh. Tech.*, vol. 41, no. 4, pp. 461–468, November, 1992.

[7] P. Höher and J. Lodge, "Iterative decoding/demodulation of coded DPSK systems," in *Proc. IEEE Global Telecommun. Conf. (Globecom)*, Sydney, Australia, Nov. 1998, pp. 598–603.

[8] N. Chotikakamthorn and H. Suzuki, "On identifiability of OFDM blind channel estimation," in *Proc. IEEE Vehicular Tech. Conf.*, Amsterdam, The Netherlands, September 1999, pp. 2358–2361.

[9] G. J. Foschini, R. D. Gitlin, and S. B. Weinstein, "Optimization of two-dimensional signal constellations in the presence of gaussian noise," *IEEE Trans. on Comm.*, vol. 22, no. 1, pp. 28–38, January, 1974.

[10] S. Y. L. Goff, "Signal constellations for bit-interleaved coded modulation," *IEEE Trans. on Information Theory*, vol. 49, no. 1, pp. 307–313, January, 2003.

[11] F. Sanzi, S. Jelting, and J. Speidel, "A comparative study of iterative channel estimators for mobile OFDM systems," *IEEE Trans. on Wireless Comm.*, vol. 2, no. 5, September, 2003.

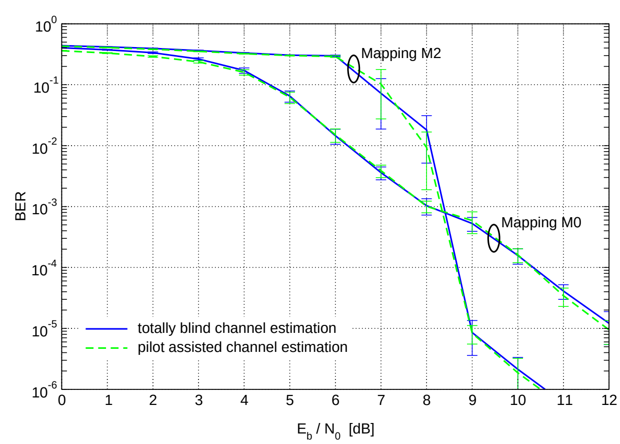

Fig. 6: Comparison of BER for blind APP-CE and pilot-aided APP-CE, both after 3 iterations.